Lab 2: Group 9

SD2231 – Applied vehicle dynamics control

May 3, 2022

Guglielmo Nappi
Lokesh Palla

Postal address	Visiting address	Telephone	Internet
Royal Institute of Technology	Teknikringen 8	+46 8 790 6000	www.ave.kth.se
KTH Vehicle Dynamics	Stockholm	**Telefax**	
SE-100 44 Stockholm		+46 8 790 9304	
Sweden			

Contents

1 Introduction

This project is intended to study the vehicle lateral slip angle by a deep comparison between a true value, measured on board the vehicle by means of the GPS and the Inertial Measurement Unit (IMU) and compared with the value computed by the designed estimators. Four different tests will be performed to be able to design good models that can accurately predict the vehicle side slip angle under different conditions such as: constant radius cornering, slalom at 30 km/h, high speed step steer and frequency sweep.

2 Task 1: Washout filtering approach of side-slip estimation

The first part of this task is dedicated to the design of the washout filtering estimator for the vehicle side-slip angle computation. The latter is a filter that processes the values of the bicycle model and the kinematic model estimators, based on a mathematical equation able to derive the vehicle side slip angle. Both two methods have strengths and weaknesses, that are combined in the washout filter to obtain the most accurate mathematical model.

2.1 Task 1.a: estimators design

The first task is to design the vehicle side-slip angle estimators architecture based on mathematical equations. To do so, it will be defined a Simulink model that, by means of the vehicle parameters and the equations, is able to draw the behaviour of the vehicle side-slip angle under the different test conditions.

2.1.1 Model-based vehicle side-slip angle estimator

The model-based estimator is based on the computation of the body side-slip angle from the bicycle model [1]. The architecture gets as input the vehicle longitudinal speed v_x, considered constant for the steady state assumption, the tyre cornering stiffnesses (C_f: cornering stiffness for the front axle, C_r: cornering stiffness for the rear axle), the vehicle mass m, the steer angle δ and the distance between the front axle and the centre of gravity (l_f) and the distance between the rear axle and the centre of gravity (l_r).

Once obtained the vehicle parameters as inputs, the estimator computes the body lateral speed based on the following equation:

$$v_y^{mod} = \frac{v_x(l_r(l_r + l_f)C_{12}C_{34} - l_f C_{12} m v_x^2)}{(l_r + l_f)^2 C_{12}C_{34} + m v_x^2 (l_r C_{34} - l_f C_{12})} \cdot \delta \qquad (1)$$

Once computed the body lateral speed for each timestep of the test, the body side-slip angle is obtained following equation (2):

$$\beta_y^{mod} = \frac{v_y^{mod}}{v_x} \qquad (2)$$

Equation (2) is obtained considering the small angle approximation, for which the tangent of the angle is equal to the angle for small angles and considering that the longitudinal vehicle slip is much larger than the body lateral speed. Figure 1 shows the architecture implemented in Simulink to obtain the body side-slip angle:

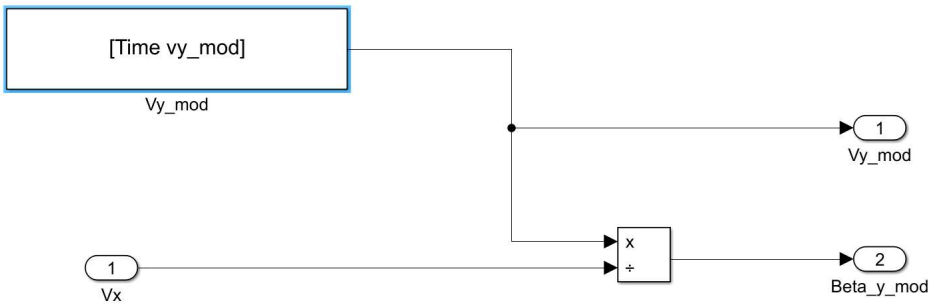

Figure 1. Bicycle model body side-slip angle estimator.

The architecture gets as input the lateral speed values computed following equation (1) and the longitudinal speed for the computation of the body side-slip angle.

2.1.2 Body side-slip by integrating lateral acceleration

A second approach for the body side-slip angle computation is to draw a model based on the integration of the lateral acceleration measured by the IMU. With this method, the vehicle lateral velocity can be easily computed by integration of two main contributions: the lateral acceleration (a_y) and the yaw velocity ($\dot{\Psi}_z$), as visible in equation (3):

$$v_y^{kin} = \int_0^T (a_y(1 - K_{roll}) - \dot{\Psi}_z v_x) dt \qquad (3)$$

Equation (3) defines the vehicle lateral speed at the IMU, it is then needed to perform a coordinate transformation to obtain the lateral speed at the centre of gravity. To do so, equation (4) is introduced:

$$v_y^{CoG} \approx v_y^{IMU} + r_x \dot{\Psi}_z - r_y \dot{\Psi}_z \quad (4)$$

Where r_x and r_y are the distances between the IMU and the centre of gravity in the longitudinal and lateral direction respectively. After defining the lateral speed in the centre of gravity, the body side-slip angle is computed following the equation (2). Once defined the equations, one can build the Simulink model, reported here in figure 2:

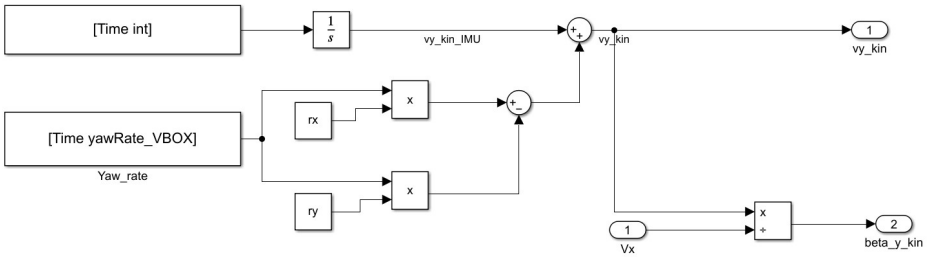

Figure 2. Kinematic model body side-slip angle estimator.

The estimator takes as input the longitudinal speed and the yaw rate from the IMU, the integrating equation useful to define the lateral speed after the integration block and the IMU coordinates with respect to the Centre of gravity. The outputs of the estimator are the lateral speed computed at the centre of gravity and the body side slip angle.

2.1.3 Washout filter for the body side-slip angle computation

The implementation of a washout filter is useful to merge the good qualities of the two models introduced before and limit their disadvantages. In particular, the bicycle model provides good estimation for the body side-slip angles at steady state whereas at transient condition, large errors are expected between the model and the true value, and the kinematic model is suffering from drift. To merge the information from both methods, it is introduced a low pass filter for the bicycle model and a high pass filter for the kinematic model, accordingly to the following equation:

$$v_y = \frac{1}{1+sT} \cdot (v_y^{mod} + sT v_y^{kin}) \quad (5)$$

Where s is the Laplace variable and T the filtering time coefficient that defines the balance between the contribution of the integral and the bicycle model. By tuning the value of it is possible to obtain a more precise observer using the washout filter with respect to the previous models. Figure 3 shows the implementation of the washout filter in Simulink:

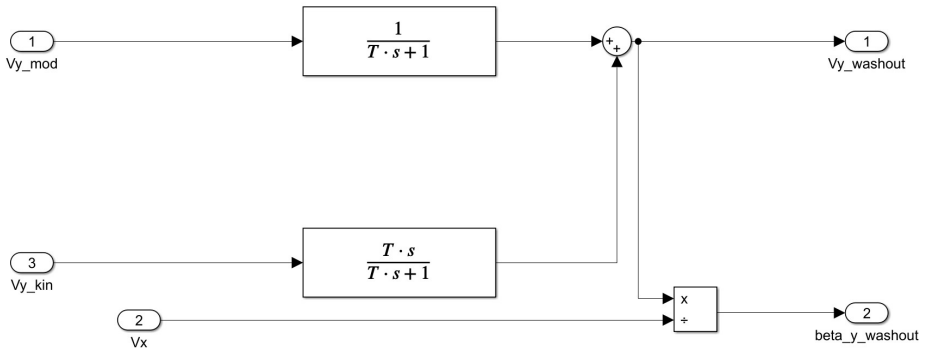

Figure 3. Washout filter body side-slip angle estimator.

The Model takes as input the model and the kinematic based lateral speed and applies the transfer function of a low pass filter and a high pass filter respectively to obtain the best observer. In the end the body side slip angle is computed by dividing the lateral speed by the longitudinal speed accordingly to the same assumptions made for equation (2).

2.2 Task 1.b: Tuning of the vehicle parameters

This section is dedicated to the tuning of the vehicle parameters, to find more accurate results of the model with respect to the real vehicle. To understand the effectiveness of the tuning, it will be analysed the maximum error and the mean squared error (MSE) between the modelled body side-slip angles and the true value according to the following equations:

$$Max\ error\ =\ max(|\beta_{true} - \beta_{model}|) \tag{6}$$

$$MSE\ =\ \frac{1}{n} \cdot sum((\beta_{true} - \beta_{model})^2) \tag{7}$$

Where β_{true} represent the true body side slip angles at each time and β_{model} the modelled one, and n is the number of measured data for the mean squared error. The approach will take care of which parameters influence the most the estimations and that have to be changed to get a better model.

The bicycle model, according to equation (1) is influenced by: the cornering stiffness of the front (C_f) and rear axle (C_r), the vehicle mass (m), the distance between the front axle and the centre of gravity (l_f) and the distance between the rear axle and the centre of gravity (l_r) and, finally, the steering gear ratio (K_s). The Vehicle used for these tests is the Volvo S90, the centre of gravity position of the vehicle is already found, and its position is here considered as correct, while the cornering stiffnesses, both for front and rear axle, are the parameters that require more accurate tuning. To do so, it is considered that the vehicle should maintain an understeering behaviour as close as possible to the neutral steering condition, obtained by the analysis of the understeering gradient coefficient K_{us} sign. Table 1 shows the relationship between the sign of the understeering gradient and the vehicle behaviour:

Table 1. Relation between understeering gradient sign and vehicle behaviour

K_{us} sign	Vehicle Behaviour
$K_{us}<0$	Oversteering
$K_{us}=0$	Neutral steering
$K_{us}>0$	Understeering

The challenge is to find a relation between the front axle cornering stiffness and the rear axle one that ensures an understeering behaviour as close as possible to the neutral steering condition. To obtain this result, equation (8) is used as a relationship between the centre of gravity position and the axle cornering stiffnesses:

$$Sign(K_{us}) = Sign(C_r \cdot l_r - C_f \cdot l_f) \tag{8}$$

In this way it is obtained that the best combination of cornering stiffnesses to reduce the maximum error and the mean squared error is reported below in table 2:

Table 2. Optimised parameters for the front and rear axle cornering stiffness

Default parameters	Optimised parameters
$C_f = 100 \cdot 10^3$ N/rad	$C_f = 109.54 \cdot 10^3$ N/rad
$C_r = 100 \cdot 10^3$ N/rad	$C_r = 140 \cdot 10^3$ N/rad

These values are obtained after performing several simulations to find the best combination of error reduction in each test. Here is reported the analysis of the improvement in terms of error reduction between the body side-slip angle measured at the IMU and the value obtained by the model. Table 3 shows the errors, both for the default parameter and the optimised version, and the percentage of error reduction for each test:

Table 3. Bicycle model observer performance with optimised parameters

	Default parameters		**Optimised parameters**		**% Reduction**	
	Max error	MSE	Max error	MSE	Max error	MSE
Test 1	0.063	0.0012	0.059	3.32e-4	05.1%	72.3%
Test 2	0.016	3.82e-5	0.009	1.30e-5	40.5%	65.9%
Test 3	0.366	0.0038	0.227	0.002	38.0%	47.4%
Test 4	0.165	0.0030	0.103	0.001	66.7%	66.7%

Another parameter that can be tuned is the roll gradient that affects the kinematic observer, and it may not be accurately measured. To best tune this parameter, it will be implemented the same approach as for the cornering stiffnesses by analysing the error between the body side-slip angle computed with the kinematic observer and the true value measured by the IMU. After trying different roll gradient values, it is seen that the default parameter already provides the best performances in terms of error for the four tests, so it is decided to keep that unchanged.

2.3 Task 1.c: Filter coefficient tuning

This section is dedicated to the tuning of the filter parameter T, value useful in the definition of the washout filter model to have the right balance between the kinematic and bicycle model to obtain a body side-slip angle more similar to the one measured by the IMU. For now, the value of the filter parameter is constant in time and it is adopted the same value for each test, meaning that it is necessary to find a good compromise to allow a good model for each condition. The process starts by defining a standard value of the filter parameter (being T=1s) used as a comparison to understand how effective the change of this parameter is on the maximum error and the mean squared error. Table 4 shows the reference errors for the tuning:

Table 4: max error and mean squared error for the standard filter parameter

T=1s	Max error	Mean squared error
Test 1	0.0066	4.31e-4
Test 2	0.4460	1.70e-3
Test 3	0.0283	6.22e-4
Test 4	0.1082	3.26e-4

Once obtained the errors for the standard filter parameter, it is time to tune the latter to obtain a compromised value to get low errors for each test. It is proven that by increasing the filter parameter, the mean squared error increases for each of the tests but decreases for test 3, if one reduces the filter parameter, the behaviour of the error is inversed. Keeping this premise in mind, it is decided to set the tuning parameter so that for each test the order of magnitude of the MSE is the same. Table 5 shows the MSE for each test and the percentage of improvement obtained with the optimal value:

Table 5: mean squared error and percentage of improvement for the optimised filter parameter

T=0.7	Mean squared error	% Improvement
Test 1	3.72e-4	13.3 %
Test 2	8.16e-4	52.0 %
Test 3	8.76e-4	-40.8 %
Test 4	2.41e-4	26.1 %

As stated, it is reached a satisfying result as the MSE error reached the same order of magnitude for each test. For what concerns the maximum error, this remains unchanged if one varies the filter parameter, hence it is not reported in table 5. In conclusion of this section, it is decided to plot the behaviour of the body side-slip angle of each model with respect to the measured value (“true” value) by the IMU for each of the 4 tests in figure (4), (5), (6) and (7):

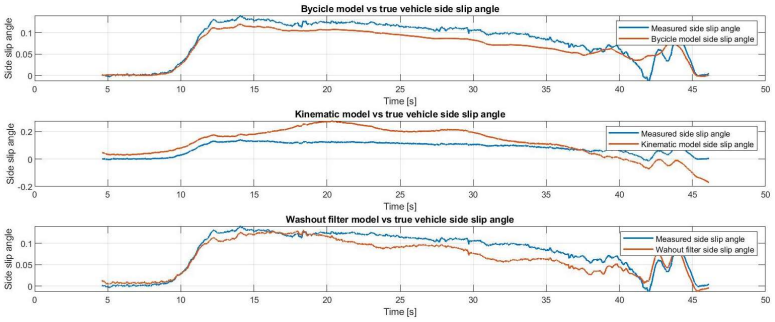

Figure 4. Constant radius cornering body side slip angle: Bicycle model (top), kinematic model (middle) and washout filter model (bottom)

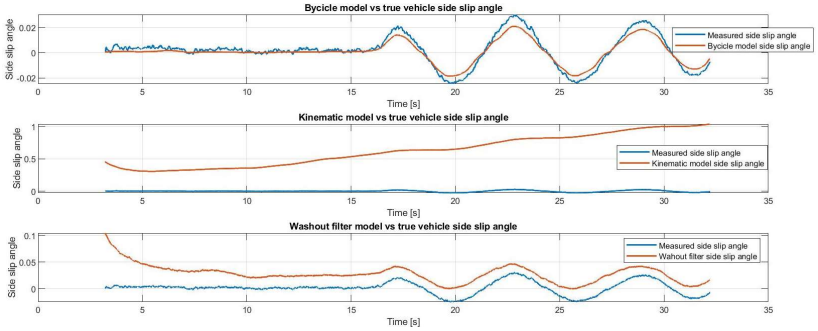

Figure 5. Slalom at v=30km/h body side slip angle: Bicycle model (top), kinematic model (middle) and washout filter model (bottom)

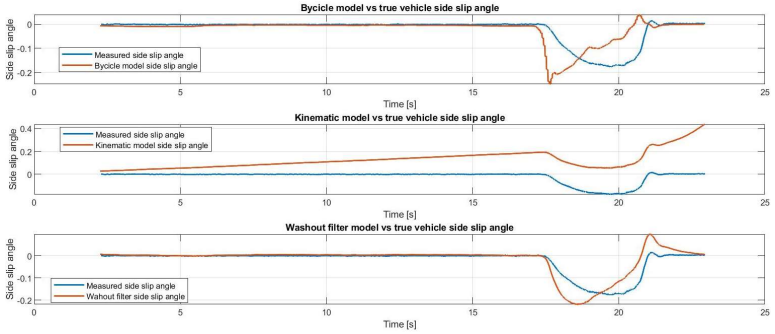

Figure 6. Step steer at v=100km/h body side slip angle: Bicycle model (top), kinematic model (middle) and washout filter model (bottom)

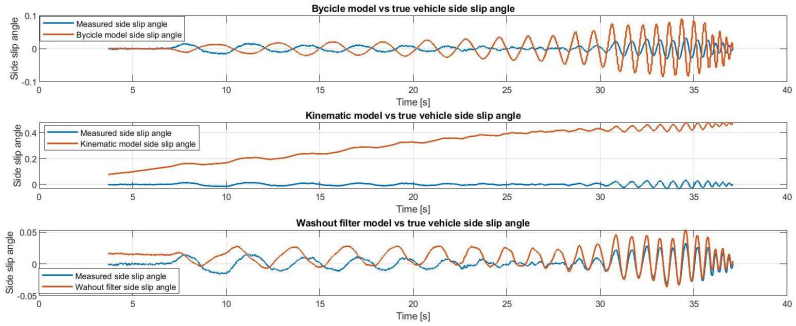

Figure 7. Frequency sweep at v=50km/h body side slip angle: Bicycle model (top), kinematic model (middle) and washout filter model (bottom)

As visible from each plot, the implementation of the washout filter reduces the differences between the measured body side-slip angle and the modelled ones, guaranteeing a better performance of the model.

2.4 Task 1.d: Quality of the body side-slip estimators

Once the vehicle and the filtering parameters are finely tuned, it is time to provide a comparison between the errors of the three estimators to understand the effective discrepancies between the true measurements and the estimated ones for each test. To do so, both maximum error and mean squared error are analysed following equation (6) and (7). Firstly, the maximum error will be analysed and compared, it will follow the analysis regarding the mean squared one. Table 6 shows the results in terms of maximum error for each test for the three estimators with respect to the true measurement:

Table 6: Max error for the three estimators for each test

	Bicycle model	Kinematic model	Washout filter
Test 1	0.0594	0.1756	0.0422
Test 2	0.0094	1.0442	0.1032
Test 3	0.2267	0.4336	0.0954
Test 4	0.1030	0.4728	0.0340

As visible from table 6, the maximum error in the washout filter is lower than the one obtained with the bicycle model observer in each test except test 2. This good result is feasible with the implementation of the kinematic model observer that allows the reduction of the maximum error for most of the driving conditions. Table 7 reports the values obtained for the mean squared error between the three estimators and the true measured body side-slip angle for each test:

Table 7: Mean squared error for the three estimators for each test

	Bicycle model	Kinematic model	Washout filter
Test 1	3.32e-4	6.60e-3	3.72e-4
Test 2	1.30e-5	4.46e-1	8.16e-4
Test 3	2.00e-3	2.83e-2	8.76e-4
Test 4	1.00e-3	1.08e-1	2.41e-4

Looking at the results in table 7, one can see that the washout filter observer ensures a great improvement in term of mean squared error both for test 3 and 4, while only in test 2 the mean squared error is increased as already happened for the maximum error. This is probably due to the steady state condition of the slalom test, that is better modelled with the bicycle model, and the implementation of the kinematic observer when defining the filter reduces the accuracy of this specific result.

2.5 Task 1.e: Understanding of the results

The purpose of this section is to understand how the three estimators drift with respect to the true measurement performed with the IMU. Firstly, it will be analysed the drifting over time, understanding how the three estimators differ from the true measurement as the time proceeds, afterwards it is important to study the observer drifting with respect to the steady state and transitioning behaviour of the vehicle and, finally, how is the observer accuracy when the speed increases. Test 1 is a reliable test to understand the accuracy of the estimators in the steady state behaviour:

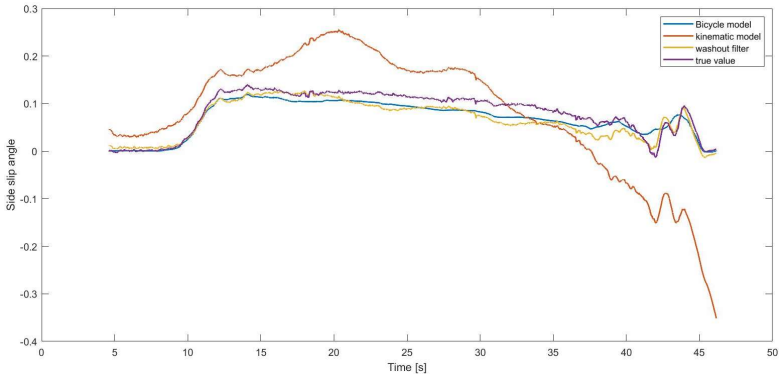

Figure 8. Estimators body side-slip angles with respect to the true measurement in constant radius cornering test

As visible from figure 8, the bicycle model estimation (blue line) provides a good estimation of the body side-slip angle in steady state conditions as the model is built to be extremely reliable under these conditions. The kinematic estimator (red line) shows an offset drift at the beginning of the measurement and tends to increase the drift over time, to appreciate more this last characteristic, test 3 is considered for a more clear analysis:

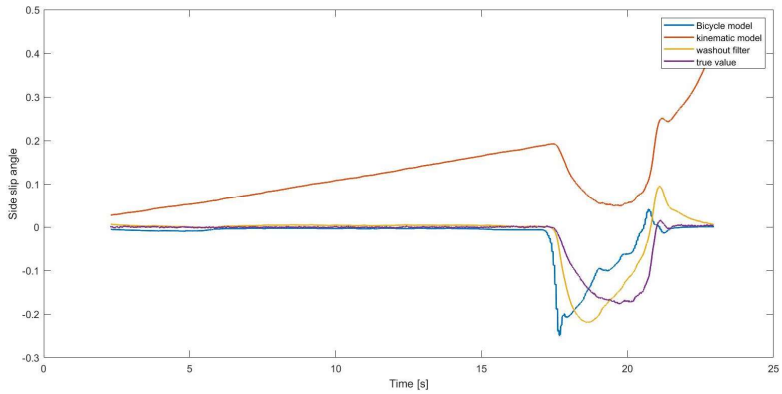

Figure 9. Estimators body side-slip angles with respect to the true measurement in step seer test at 100 km/h

As visible from figure 9, the kinematic observer tends the most to drift over time with respect to the true body side-slip angle measured by the IMU (purple line). The kinematic observer tends to a span drift, where the error increases proportionally with time but it is not affected by the step steering manoeuvre.

For what concerns the bicycle model observer, one can observe that in a transitioning manoeuvre, the model provides a zonal drift with respect to the true value that representing the initial hypothesis to accurately model the body side-slip angle only in steady state conditions. Both in test 1 and 3, the washout filter observer (yellow line), is the one that provides the lowest drift with respect to the measured value as it provides a more accurate behaviour both in transitioning and steady state behaviour and it is the one that tends the least to drift over time. To understand the estimators drifting over speed, test 4 is analysed as follows:

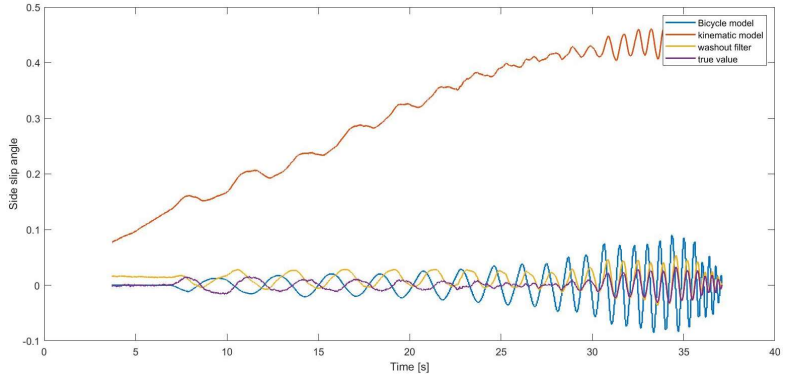

Figure 10. Estimators body side-slip angles with respect to the true measurement in frequency sweep at 50 km/h

Figure 10 indicates that the bicycle model drifting is reduced with the speed, as visible in the beginning of test 4, with respect to the one obtained in test 3. Moreover, it is visible how, the bicycle model tends to drift more over time as the vehicle tends to lose the steady state behaviour. Test 4 confirms as well how the kinematic model is strongly affected by the drifting over time but less on the vehicle behaviour and speed. To obtain a more precise observer, one can try to define a linear filtering coefficient that gives more weight to the bicycle model under steady state conditions and increases the weight of the kinematic model under transitioning behaviour.

2.6 Task 1.f: Linear filter coefficient

This task is intended to modify the washout filter parameter to obtain more reliable results. Up to now, the filtering coefficient is set as constant for each driving conditions which can give less precise results especially in transitioning conditions. The objective now, is to draw an equation that allows a dependency of the filtering coefficient on the vehicle behaviour, so that in case of steady state manoeuvres, more weight is put on the bicycle model, while under transitions, allows the kinematic model to be preponderant. It is decided to take the lateral jerk measured by the IMU to be the indicator of vehicle stability, it is predictable that under low lateral accelerations rate change, the vehicle is in steady state condition, while under larger jerk this state is lost. Following this brief introduction, the filtering parameter is modelled as follows:

$$T = \text{proportional} \cdot \left| \dot{a}_{y\_CoG} \right| + offset \qquad (9)$$

Equation (8) shows the filter parameter linear characteristic that depends on the vehicle lateral acceleration rate of change as an indication for the vehicle behaviour. It is decided to introduce the absolute value of the jerk to avoid negative filtering times, that would disallow the correct functioning of the filter, and an offset to guarantee a non-null filtering parameter when the lateral acceleration variation is zero. The proportional parameter is tuned by understanding the jerk order of magnitude and trying to replicate a filtering parameter that, under transient conditions, at high jerk, is close to the constant filter parameter.

Table 8. Filter equation parameters.

Proportional parameter	**Offset parameter**
Proportional = 0.04	Offset = 0.005

Once tuned the parameters, it is interesting to compare the errors between the new washout-filter and the old version with the constant tuning, to understand if effectively there is an error reduction based on the assumptions made. Table 9 shows the maximum error and the mean squared error of the new washout filter with respect to the old version with constant filtering parameter:

Table 9. Mean squared error and maximum error with the linear filtering parameter with respect to the constant model.

	Constant filtering parameter		**Linear filtering parameter**	
	Max error	MSE	Max error	MSE
Test 1	0.0422	3.72e-4	0.0587	3.23e-4
Test 2	0.1032	8.16e-4	0.0099	1.28e-5
Test 3	0.0954	8.76e-4	0.2173	1.80e-3
Test 4	0.0340	2.41e-4	0.0898	8.98e-4

The error table shows how under steady state conditions, the error is drastically reduced with the linear filter parameter, while under transient conditions the model gives poor results. This is due to the main role of the kinematic observer in the washout filter under transient conditions. Figure (11), (12), (13) and (14) aims to picture the behaviour in time of the body side-slip angle with the constant filtering parameter and the linear one in the washout model:

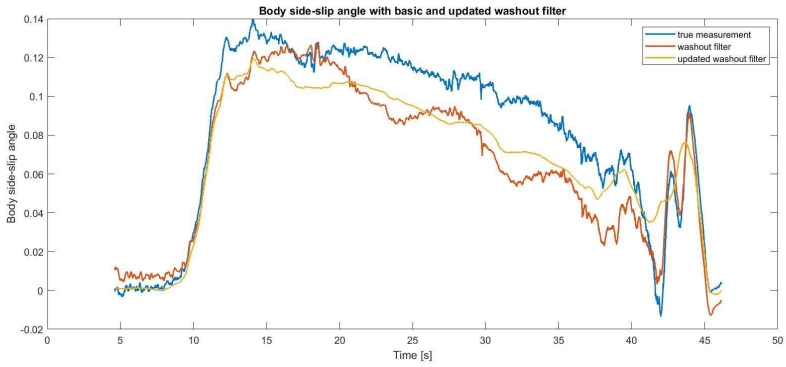

Figure 11. Constant radius cornering body side-slip angle with basic washout filter (red line), updated washout filter (yellow line) and true value (blue line)

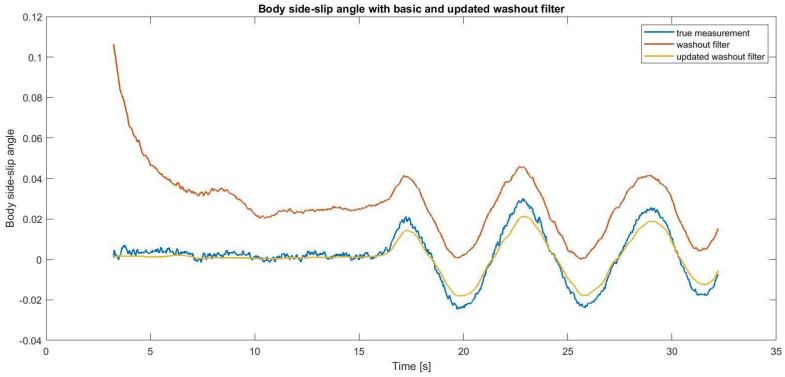

Figure 12. Slalom at v=30km/h body side-slip angle with basic washout filter (red line), updated washout filter (yellow line) and true value (blue line)

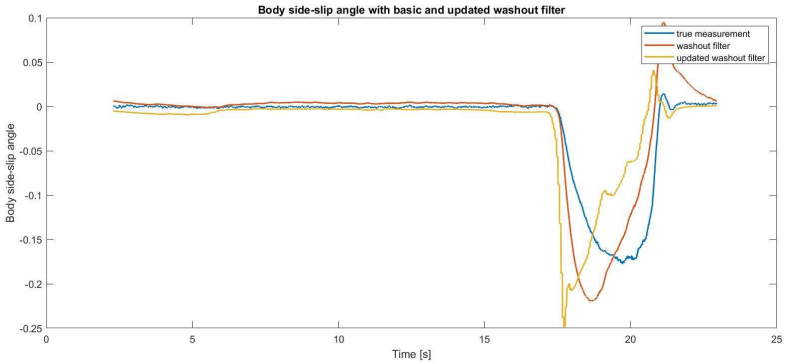

Figure 13. Step steer at v=100km/ body side-slip angle with basic washout filter (red line), updated washout filter (yellow line) and true value (blue line)

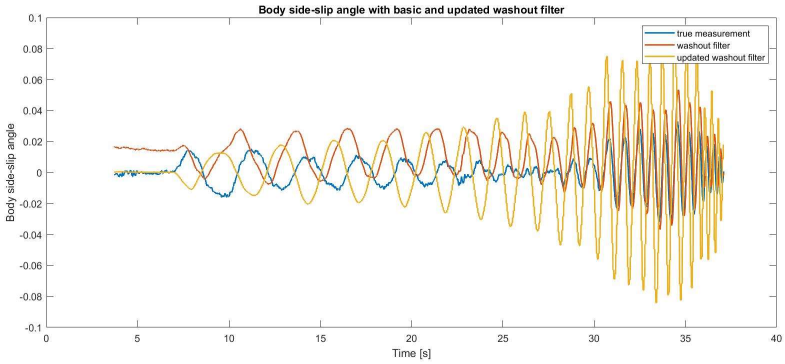

Figure 14. Frequency sweep at v=50km/h body side-slip angle with basic washout filter (red line), updated washout filter (yellow line) and true value (blue line)

As predictable, the behaviour of the updated washout filter model is extremely more precise under steady state conditions, reached at low lateral acceleration rate of change. Under transient conditions, the results are negatively affected by the large errors in the kinematic observer.

3 Task 2: Unscented Kalman filter estimation

The Unscented Kalman filter, referred in this text as UKF, is a filter that by using a set of measurements observed in time, produces an estimation of unknown variables in a nonlinear system. This algorithm can be applied to the vehicle to estimate the body side-slip angle and compare the model obtained with the UKF with the observer designed in task 1.

3.1 Task 2.a: UKF design

The Unscented Kalman filter is based on two steps, the predict step, and the update step, to produce a reliable model of a nonlinear system. The predict step produces an estimation of the current state based on measurements performed in previous time step. Once obtained the estimation, the update step combines the current step measurement to update the state estimate in the predict step [2]. It is fundamental to define which variables are state variables used in the predict step and which variables are measured to refine the estimation in the update state when modelling the body side slip-angle and defining the equations accordingly. The state variables are the longitudinal velocity (v_x), the lateral velocity (v_y) and the yaw rate ($\dot{\psi}_z$), these variables are obtained by the integration of the longitudinal and lateral acceleration and the variation of the yaw rate using the Runge Kutta of 4th order. Equations (10), (11) and (12), derive the longitudinal and lateral acceleration and the rate of change of the yaw rate from the free body diagram of a vehicle, as shown below in figure (15):

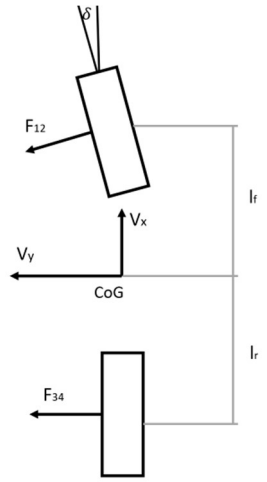

Figure 15. lateral dynamics free body diagram

$$\dot{v_x} = \frac{-F_{12}sin(\delta) + \dot{\psi}_z v_y}{m} \quad (10)$$

$$\dot{v_y} = \frac{F_{34} + F_{12}cos(\delta) - \dot{\psi}_z v_x}{m} \quad (11)$$

$$\ddot{\psi}_z = \frac{l_f F_{12}cos(\delta) - l_r F_{34}}{I_z} \quad (12)$$

Where the steering angle δ is the input parameter. Once defined the state equations, it is time to define the measurement equations useful in the update step to correct the initial prediction. The measurement variables are the longitudinal velocity, the lateral acceleration (a_y) and the yaw rate and are taken from the state of the system. To allow the UKF to work properly, it is required to arbitrarily define a system initial state that it is used by the predict step to start with the estimation. It is then decided that the initial state of the vehicle is a standing still state, where all the state variables are null. Moreover, it is important to define the initial estimation covariance for each state variable, this matrix is fundamental as it gives an initial information about the covariance of the data used to build the model. This matrix is arbitrarily defined as a diagonal matrix, where each position of the diagonal defines a reasonable covariance for the data measured by the IMU. Once the first iteration is done by the UKF, the initial state and the initial estimated covariance are updated, and the filter can build the model according to the equations over mentioned. The following figures show the UKF model of the body side-slip angle with respect to the true value measured by the IMU:

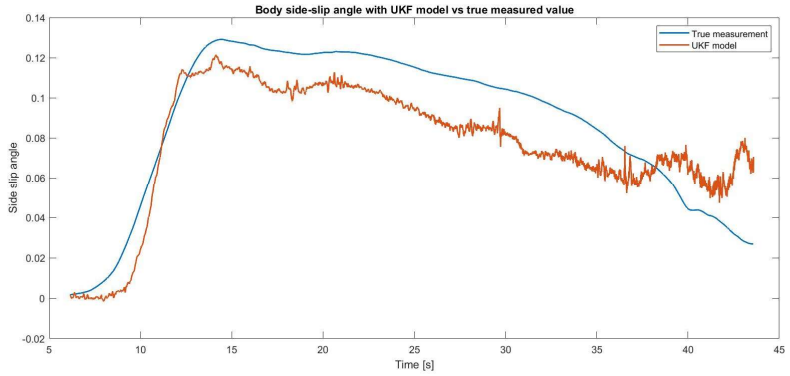

Figure 16. Constant radius cornering body side-slip angle with the UKF (red line) and the true value (blue line)

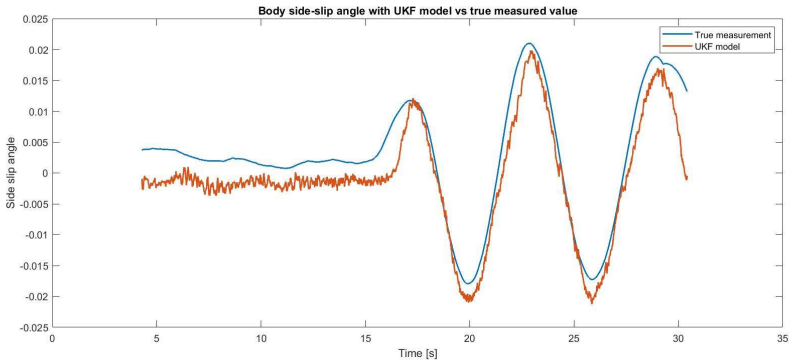

Figure 17. Slalom at v=30km/h body side-slip angle with the UKF (red line) and the true value (blue line)

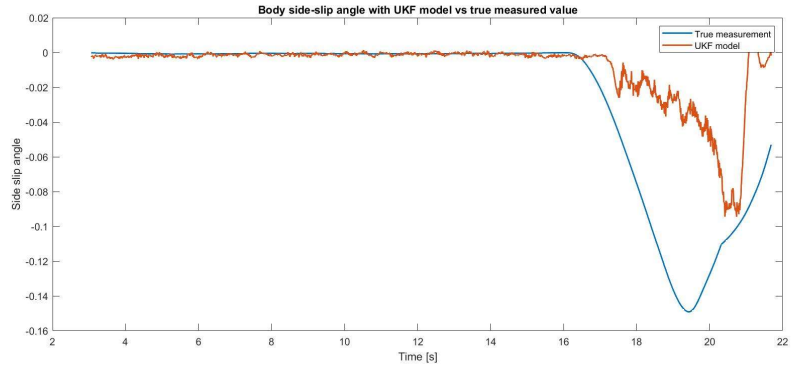

Figure 18. Step steer at v=100km/h body side-slip angle with the UKF (red line) and the true value (blue line)

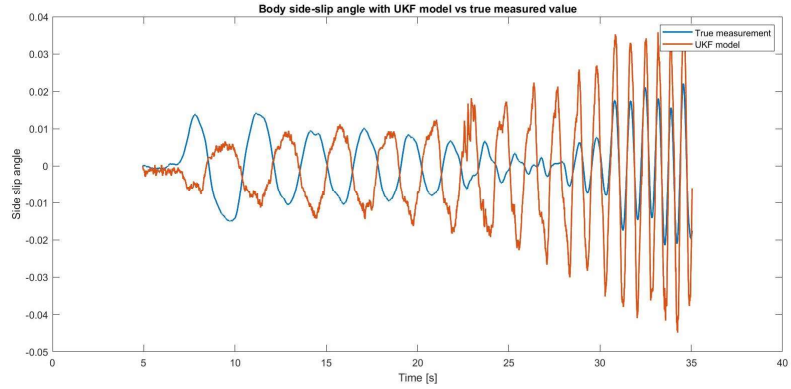

Figure 19. Frequency sweep at v=50km/h body side-slip angle with the UKF (red line) and the true value (blue line)

The UKF model, as visible shows a lot of noise in the computation of the body-side slip angle that is intended to reduce by tuning the process and measurement noise that negatively affect the body side-slip modelling. The tuning of the UKF will be performed in the following sections aiming to reduce the discrepancies between the true measurement and the filter model.

3.2 Task 2.b: UKF application

This task is intended to show the estimation performed with the Unscented Kalman filter with respect to the one obtained with the three estimators designed in task 1. The performances are evaluated for each of the four tests, and it is expected to obtain a more accurate result with respect to the "true" measurement of the IMU in transient behaviour. Figure (20), (21), (22), and (23) shows the behaviour of the UKF model with respect to the body-side slip angle estimators previously modelled:

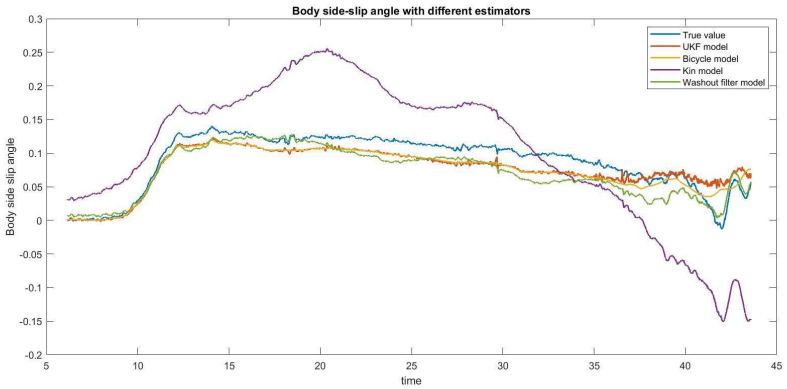

Figure 20. Constant radius cornering body side-slip angle with the UKF (red line), the true value (blue line), Bicycle model (yellow line), kinematic model (purple line) and washout filter model (green line)

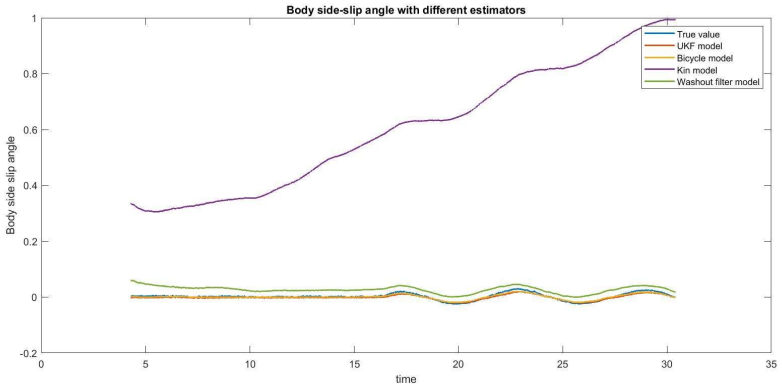

Figure 21. Slalom at v=30km/h body side-slip angle with the UKF (red line), the true value (blue line), Bicycle model (yellow line), kinematic model (purple line) and washout filter model (green line)

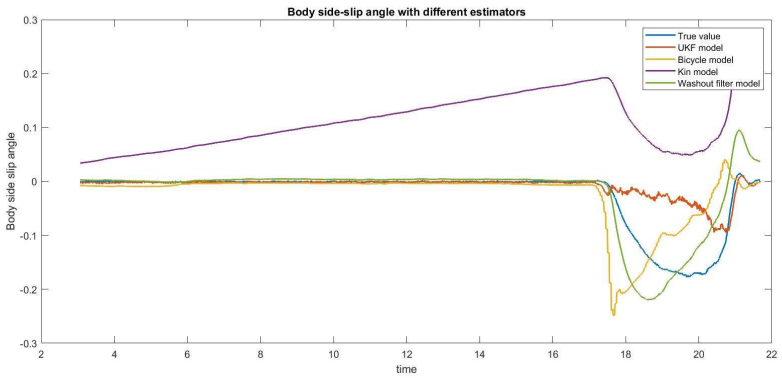

Figure 22. Step steer at v=100km/h body side-slip angle with the UKF (red line), the true value (blue line), Bicycle model (yellow line), kinematic model (purple line) and washout filter model (green line)

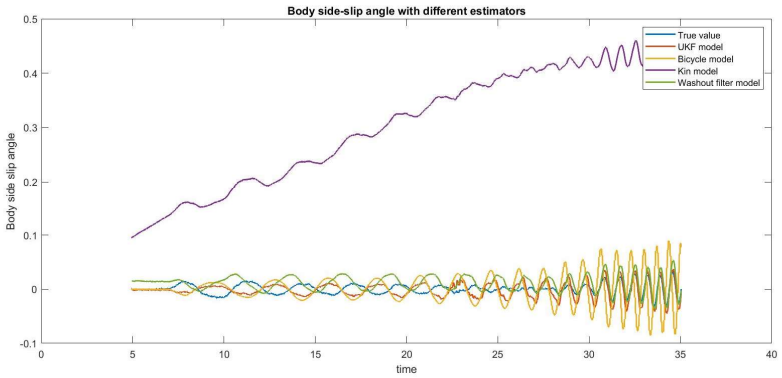

Figure 23. Frequency sweep at v=50km/h body side-slip angle with the UKF (red line), the true value (blue line), Bicycle model (yellow line), kinematic model (purple line) and washout filter model (green line)

As predicted, the UKF model allows a better description of the body side-slip angle under transient conditions, while it is less precise when it comes to model the steady state behaviour due to the high process and measurement noises. By tuning the UKF noise covariance matrices and the transformation parameters it will be possible to reduce the error under steady state conditions as well.

3.3 Task 2.c: UKF model tuning

Within this task it is intended to tune the parameters that affects the modelling of the body side-slip angle when implementing the Unscented Kalman filter. In particular, it is important to tune the covariance and the process noise to reduce the errors and the transformation parameters that affects the predict and update step (alfa, beta and kappa) to obtain a better tuning of the model. To have a fair comparison with the un-tuned UKF model, it is decided to compute the mean squared error and the maximum error between the modelled beta and the one measured with the IMU. Table 10 shows the process and measurement noise covariance matrices with the default values and the optimised ones:

Table 10. Process and measurement noise covariance matrices with default values and tuned values

	Default values			**Tuned values**		
Process noise covariance matrix	0.1	0	0	$2.406e$-5	0	0
	0	0.1	0	0	$2.406e$-5	0
	0	0	0.1	0	0	$1e$-6
Measurement noise covariance matrix	0.01	0	0	0.1	0	0
	0	0.01	0	0	0.1	0
	0	0	0.01	0	0	0.1

As visible the covariance matrices are diagonal matrices where each non null value represents the covariance computed for each of the state variables, hence for the first line is the longitudinal speed, for the second line the lateral speed and the third line the yaw rate [3]. It is seen that the modification of the covariance matrices produces the largest error reduction with respect to the changes in the transformation parameters that are reported in table 11:

Table 11. Transformation parameters with default and tuned values

	Default parameters	**Tuned parameters**
Alfa	1	0.5
Beta	1	2.5
Kappa	1	0.9

Once designed the tuned UKF the mean squared error and the maximum error are computed and compared with respect to the un-tuned one to understand the effectiveness of the tuning:

Table 12. Tuning effect in terms of mean squared error and max error for each test

	Default UKF		**Tuned UKF**			
	Max error	MSE	Max error	MSE	%Max	%MSE
Test 1	0.0639	3.81e-4	0.0487	3.24e-4	23.7%	15.0%
Test 2	0.0163	1.75e-5	0.0146	1.00e-5	10.2%	42.8%
Test 3	0.1503	1.44e-3	0.0966	9.55e-4	35.7%	33.6%
Test 4	0.0503	2.44e-4	0.0333	3.17e-4	33.8%	-29.9%

As visible from table 12, the tuning of the UKF helped in reducing the maximum and the mean squared error for each test, confirming the good quality of the tuning. Only the maximum error in test 4 is increased. Figure (24), (25), (26) and (27) aims to compare the body side slip angle modelled with the tuned UKF with respect to the measured value by the IMU.

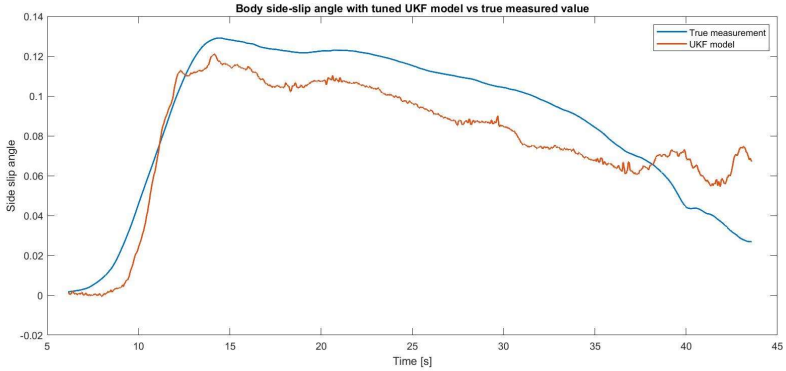

Figure 24. Constant radius cornering body side-slip angle with tuned UKF (red line) and the true value (blue line)

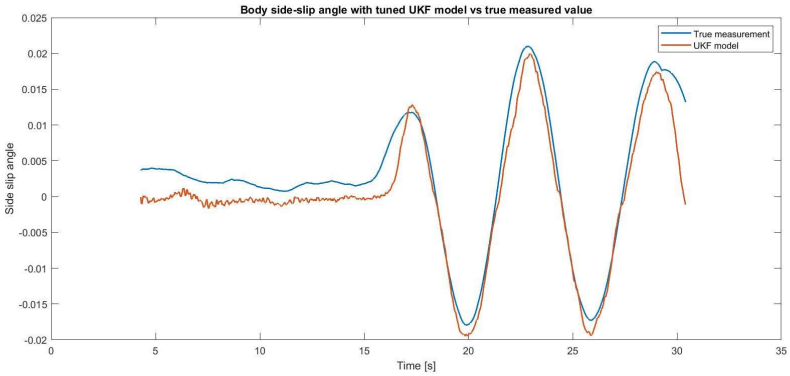

Figure 25. Slalom at V=30km/h body side-slip angle with tuned UKF (red line) and the true value (blue line)

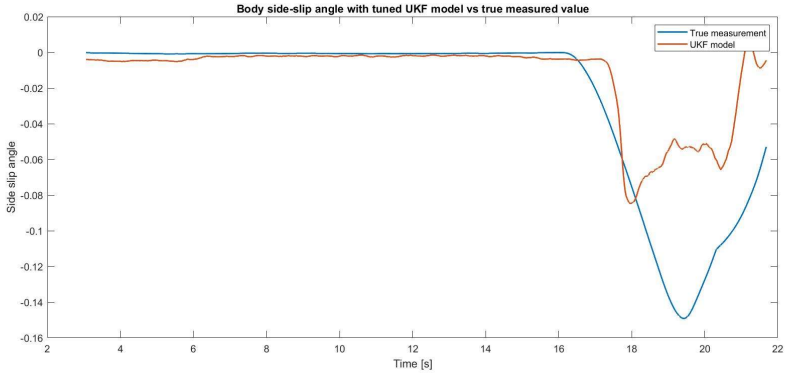

Figure 26. Step steering at V=100km/h body side-slip angle with tuned UKF (red line) and the true value (blue line)

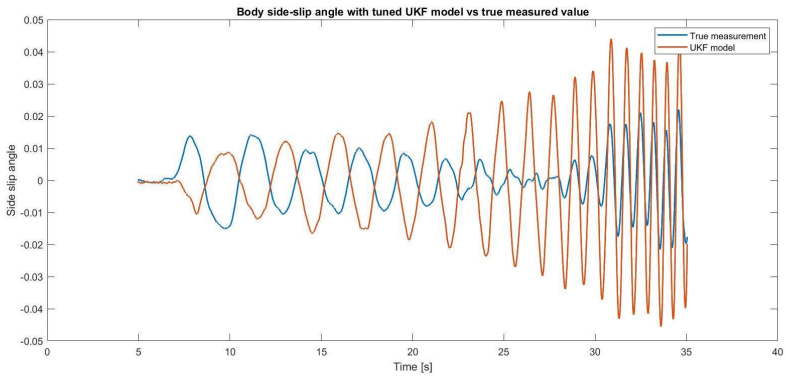

Figure 27. Frequency sweep at V=50km/h body side-slip angle with tuned UKF (red line) and the true value (blue line)

For each of the tests, the tuning positively affects the behaviour in time of the body side-slip angle model. One can confirm that by analysing the above figures as the UKF model computes a more smooth and similar body side-slip angle with respect to the untuned filter. This result confirms the quality of the tuning and the effectiveness on the results.

3.4 Task 2.d: Brush tyre model

This task is intended to extend the vehicle dynamics model by studying the vehicle parameters. In particular, it is found out that changing tyre cornering stiffness for both front axle and rear axle and vehicle roll gradient will affect the dynamic behaviour of the vehicle, by adopting a dynamic tyre model instead of a linear model. It is then considered the tire brush model, where the longitudinal and lateral force are proportional to the tyre slip up to reaching saturation. To conduct this study, it is considered a constant road friction coefficient equal to 1, value close to the one of dry tarmac. Due to tyre deformation after a period that build ups lateral force and aligning moment at small slip angles when the tyre running conditions suddenly changes. This causes the deflection due to contact between flexible bristles and road surface by the generation of slip and leads to sliding condition.

To study the lateral force generation at large slip angles, brush model of tyre is constructed analytically in the state and measurement equations where the normal force (F_z) is calculated and assumed to be evenly distributed over the contact length at a given constant vertical pressure. By Introducing variable (λ) in equation (12) as the area of adhesion zone, which specifies the relationship between the dependency of longitudinal velocity and lateral displacement of the tyre and the lateral force per tyre, the following equations are derived:

$$\lambda = \frac{\mu F_z}{2C_\alpha \tan \alpha} \tag{12}$$

$$F_y = -C_\alpha \tan \alpha \; f(\lambda) \tag{13}$$

Once defined the equation, it is important to define whether a region of the tyre is under sliding conditions or the entire contact surface between tyre and road is in adhesion condition. Equation (14) helps in defining the value of λ both for sliding and adhesion region:

$$f(\lambda) = \begin{cases} \lambda(2-\lambda) & \lambda \leq 1 \\ 1 & \lambda > 1 \end{cases} \tag{13}$$

Once the model is defined, it is implemented in MATLAB and the following results are obtained:

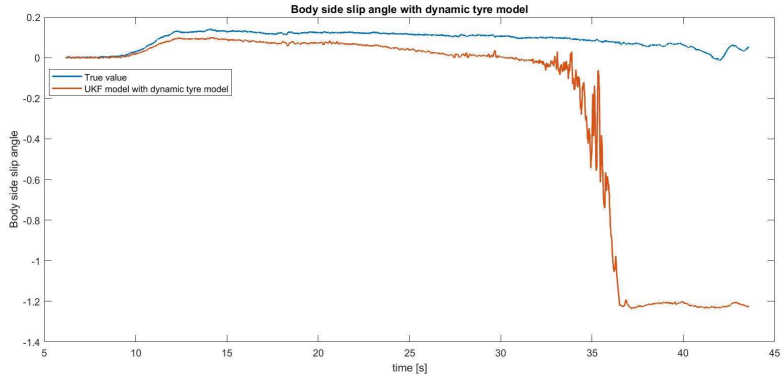

Figure 25. Constant radius cornering body side-slip angle with dynamic tyre model UKF (red line) and the true value (blue line)

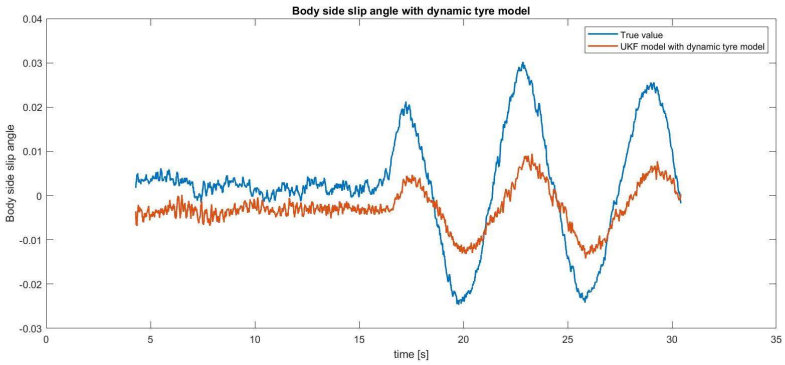

Figure 26. Slalom at v=30km/h body side-slip angle with dynamic tyre model UKF (red line) and the true value (blue line)

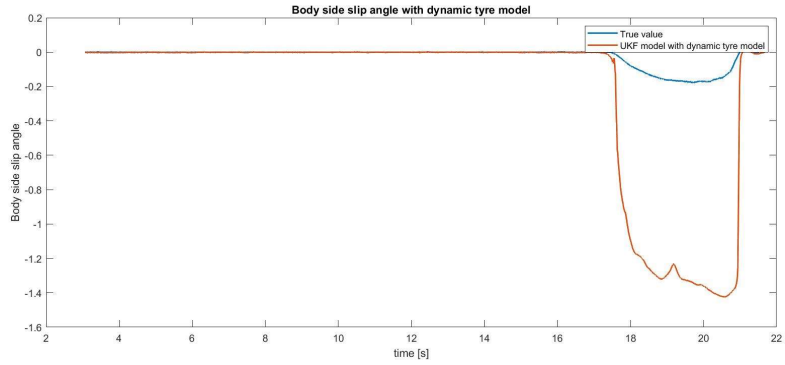

Figure 27. Step steer at v=100km/h body side-slip angle with dynamic tyre model UKF (red line) and the true value (blue line)

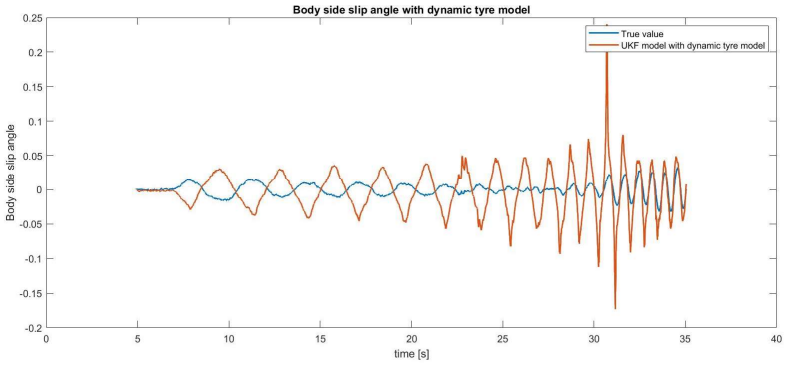

Figure 28. Frequency sweep at v=50km/h body side-slip angle with dynamic tyre model UKF (red line) and the true value (blue line)

The dynamic model introduces the sliding conditions on the tyre that may cause an overall enlargement of the body side slip angle under transient conditions when the lateral jerk is extremely high.

4 References

[1], [2] M. Nybacka, M. Jonasson, "Lab 2-Lateral Dynamics - State estimation, April 1, 2022

[3] J. Hartikainen and S. Särkä, "Optimal filtering with Kalman filters and smoothers", February 25, 2008